

**HIGGS BOSON PRODUCTION INCLUDING
ALL-ORDERS SOFT GLUON RESUMMATION**

Edmond L. Berger

Argonne National Laboratory

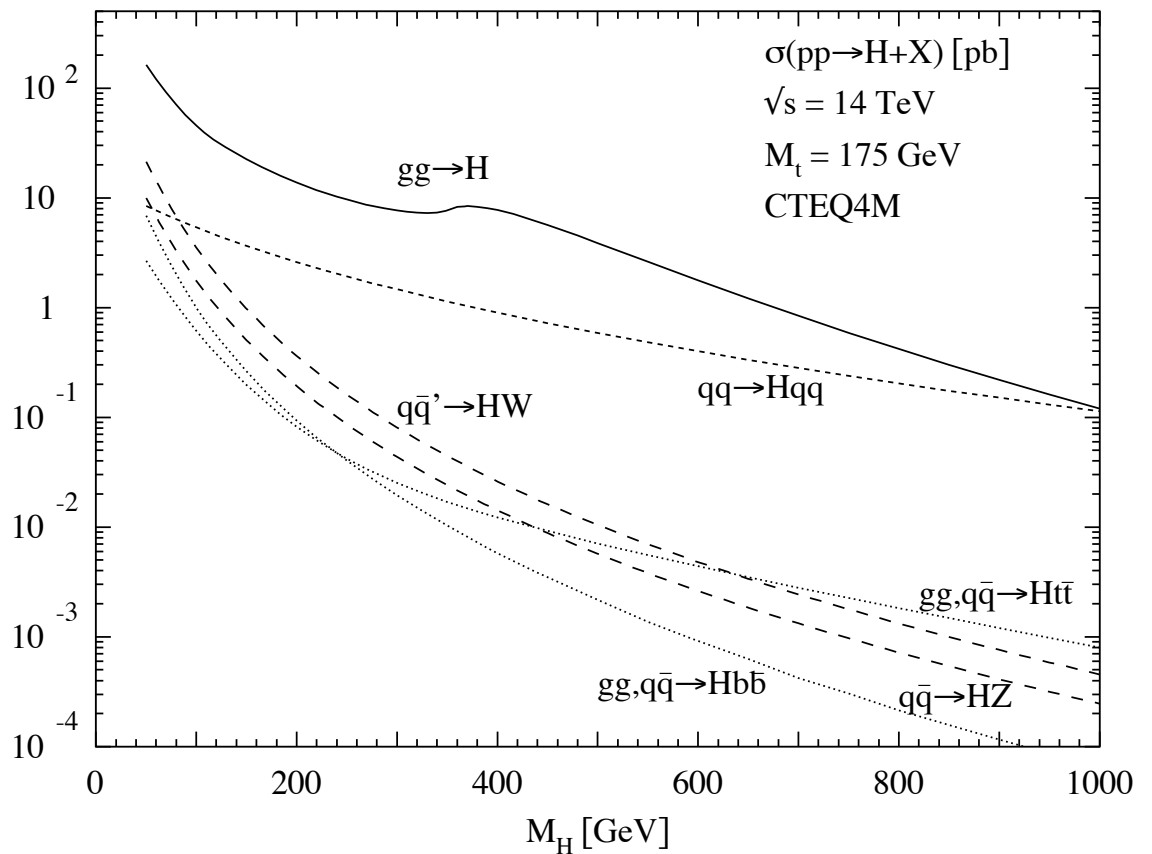
November 21, 2002

1. Higgs Boson Phenomenology at the LHC
2. Transverse Momentum Distribution
3. All orders Soft Gluon Resummation
4. Role of the Non-perturbative Input at Large Impact Parameter
5. Predictions for Transverse Momentum Distributions of Higgs and Z Bosons at the LHC
6. Summary and Discussion

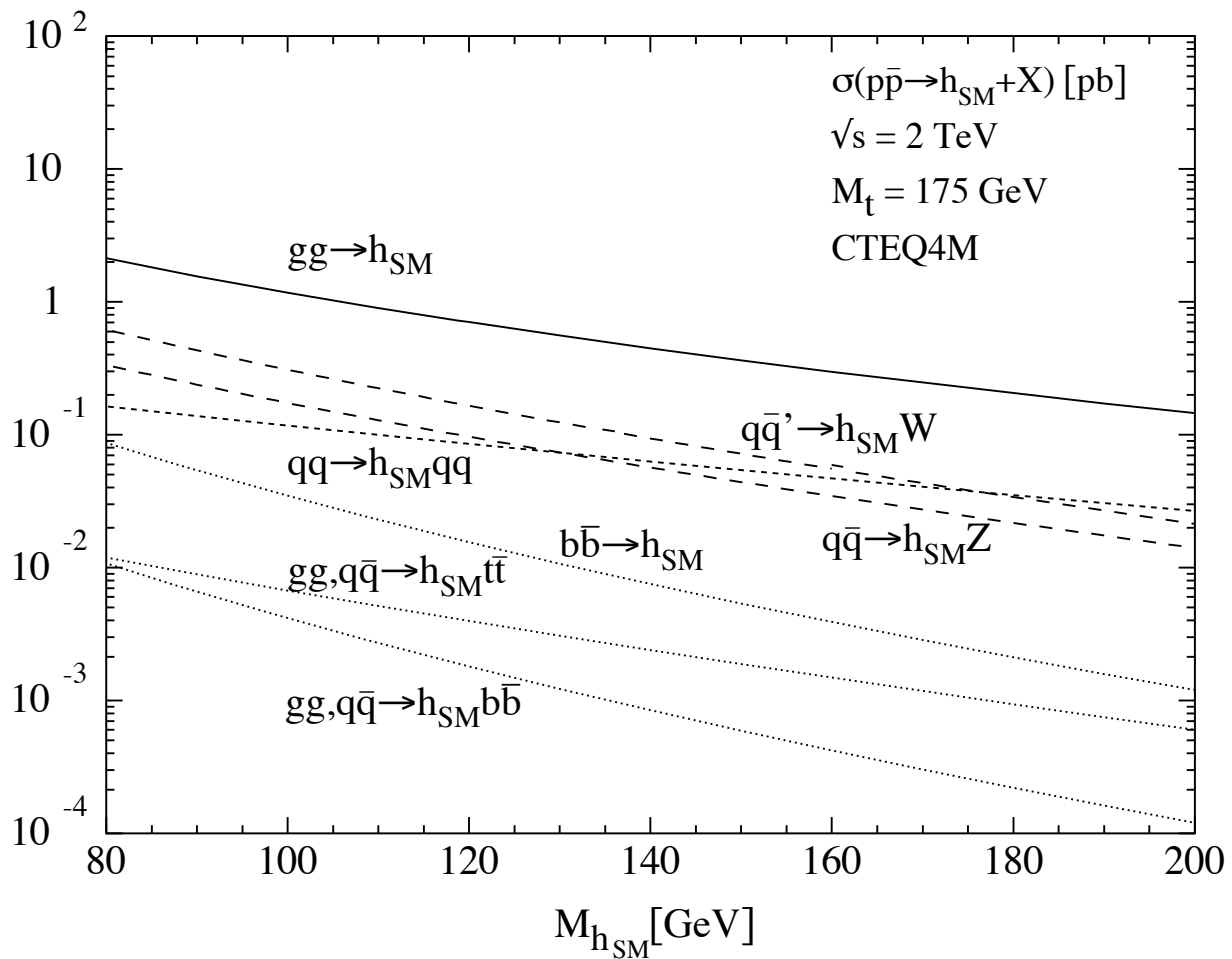
1. INTRODUCTION

- To establish the Higgs mechanism for electroweak symmetry-breaking, it is necessary to
 - discover the Higgs boson
 - demonstrate mass generation $g_{hxx} \propto m_x$
- The experimental bounds on m_h from the absence of a signal at LEP in $e^+e^- \rightarrow hZ$ are
 - $m_h > 115$ GeV if the branching fraction for decay to $b\bar{b}$ is significant
 - $m_h > 113$ GeV based on the assumption of decay into hadronic jets, without b -tagging
- Fits to precise electroweak data suggest that the mass of the scalar SM-like Higgs boson, $m_h < 193$ GeV
- In this work, we consider the broader range $M_Z < m_h < 200$ GeV
 - Interesting to contrast the transverse momentum distributions for Z and Higgs boson production at the same mass

- The Higgs boson is expected to be produced at the LHC through various partonic production processes and observed in its decays to SM particles
 - $gg \rightarrow hX$, with $h \rightarrow \gamma\gamma, h \rightarrow WW^*, ZZ^*$;
 - $gg \rightarrow t\bar{t}hX$, with $h \rightarrow b\bar{b}$ or $h \rightarrow \gamma\gamma$;
 - $qq \rightarrow hqqX$ via $W^+W^- (ZZ) \rightarrow hX$, with $h \rightarrow WW^*, h \rightarrow \gamma\gamma$, or $h \rightarrow \tau^+\tau^-$
- The fully inclusive gluon-gluon fusion subprocess $gg \rightarrow hX$ is the dominant production mechanism



TEVATRON PRODUCTION CROSS SECTIONS



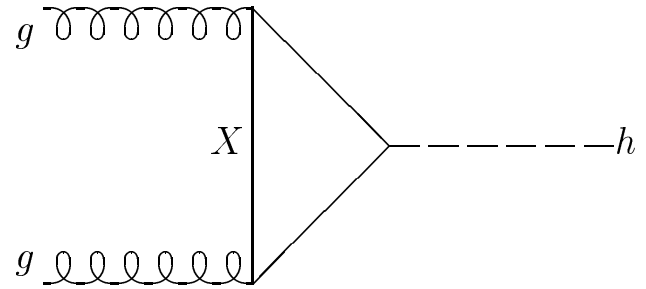
M Spira hep-ph/9810289

- Cross section is smaller than at the LHC by a factor of ~ 100 to 1000
- Combine many channels for the Higgs boson search
- Integrated luminosity of at least 20 fb^{-1} is required for discovery of a Higgs boson with $m_h = 120 \text{ GeV}$
- Associated production $q\bar{q}' \rightarrow (W, Z) \rightarrow h(W, Z)$ is important for the Tevatron search

GLUE - GLUE FUSION

- lowest order triangle graph

$$X = t, b, \tilde{q}$$



- In the SM, the top quark t contribution dominates
- Take the limit $m_t \rightarrow \infty$. The triangle collapses to a point. The predicted cross section agrees within 5% with the triangle cross section for $m_h < 2m_t$

- Effective 0th order cross section

$$\sigma_{gg \rightarrow hX}^{(0)}(Q) = \sigma_0 \frac{\pi}{S} m_h^2 \delta(Q^2 - m_h^2)$$

$$\sigma_0 = \left(\sqrt{2}G_F\right) \frac{\alpha_s^2(\mu_r)}{576\pi}$$

G_F is the Fermi constant

- The NLO contributions are large, $K_{NLO} \sim 1.7$

Spira, Djouadi, Graudenz, and Zerwas; Dawson and Kauffman

- NNLO contributions, $K_{NNLO}(m_h \ll m_t) \sim 2$

Harlander and Kilgore PRL 88, 201801 (2002); Anastasiou and

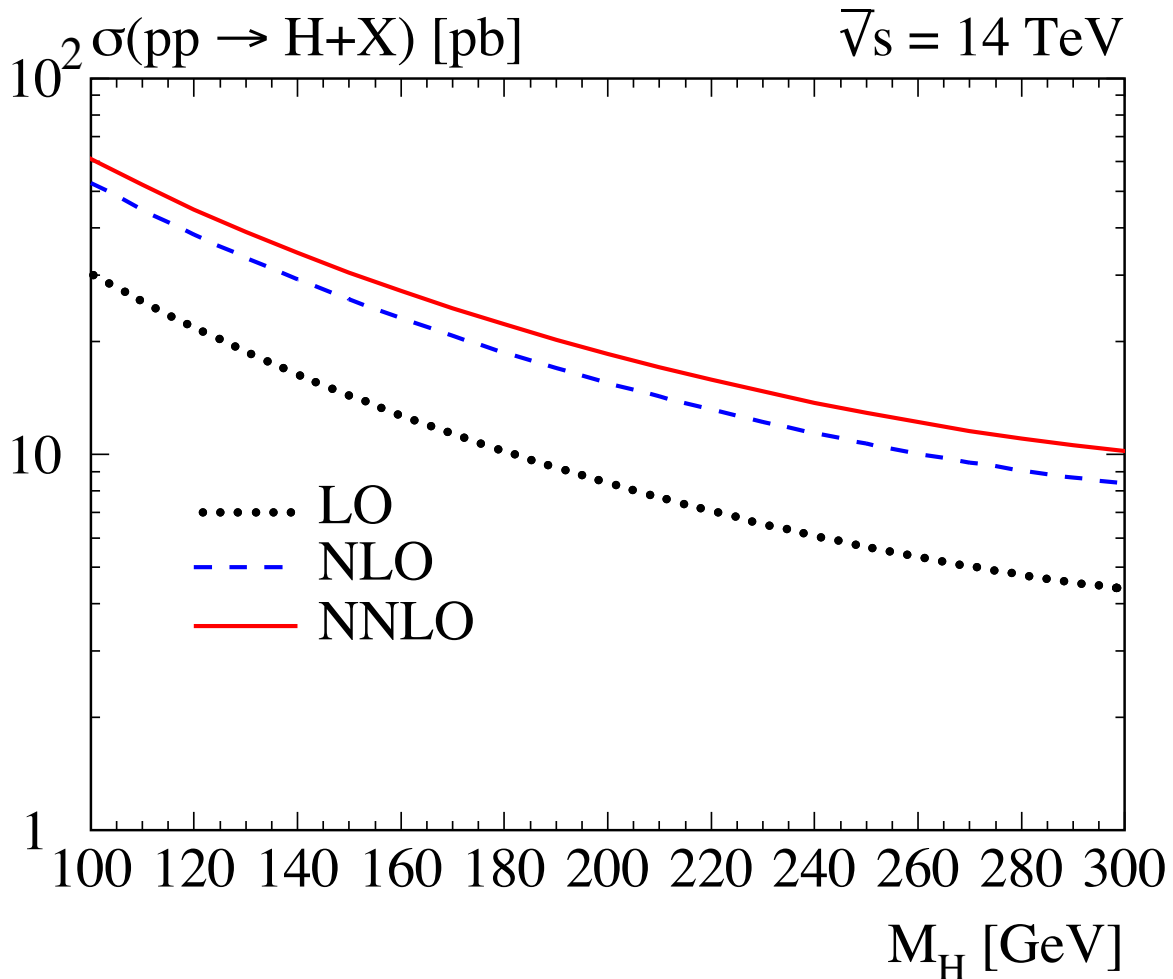
Melnikov, hep-ph/0207004

- The inclusive cross section, integrated over transverse momentum, is established; renormalization/factorization scale dependence $\sim 15\%$

TOTAL CROSS SECTION AT NNLO

- Total inclusive cross sections computed at NNLO

Harlander and Kilgore

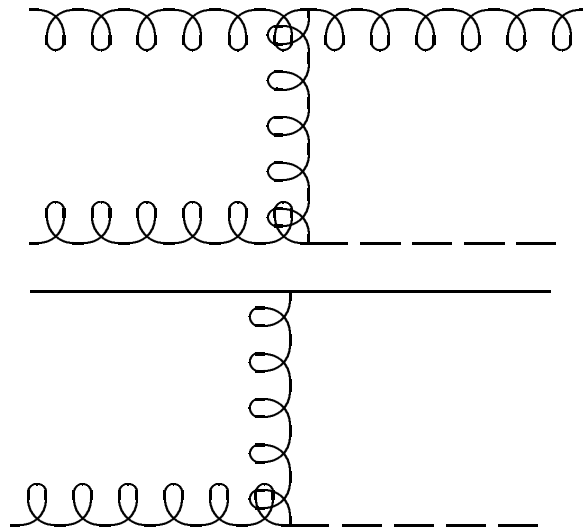


- Perturbation theory is well behaved (scale dependence is under control and growth in magnitude from NLO to NNLO is modest)
- Threshold soft gluon resummation ($m_h/\sqrt{S} \rightarrow 1$)

Catani, deFlorian, Grazzini, Nason

2. CROSS SECTION AT FINITE TRANSVERSE MOMENTUM Q_T

- At zero-th order, the triangle diagram produces a $\delta^2(\vec{Q}_T)$ -function transverse momentum distribution
- Finite Higgs boson transverse momentum is provided at order α_s by gg , qg , and $q\bar{q}$ subprocesses



– Also $gg \rightarrow g^* \rightarrow gh$ and $q\bar{q} \rightarrow g^* \rightarrow gh$

- In the limit $m_t \rightarrow \infty$, the predicted cross section agrees with the full triangle calculation within a few % if $m_h < 2m_t$ and $Q_T < m_t$

Baur and Glover NP B339, 38 (1990)

CROSS SECTION AT FINITE TRANSVERSE MOMENTUM Q_T

- Extraction of a signal for the Higgs boson is aided by an accurate expectation of the Q_T distribution
- Event modeling, kinematical acceptance, and efficiencies all depend on Q_T
- Expected shape of $d\sigma/dQ_T$ can affect experimental triggering and analysis strategies
- Selections on Q_T can be used to enhance the signal/background ratio
- In the LHC CMS detector, vertex pointing is not possible with the CMS barrel so that the behavior of $d\sigma/dQ_T$ affects the precision of the determination of the event vertex from which the Higgs boson ($\gamma\gamma$ peak) emerges. Greater Q_T activity associated with Higgs boson production allow a more precise determination of the vertex especially in the case of multiple events per beam crossing

DIFFERENTIAL CROSS SECTION AT NLO

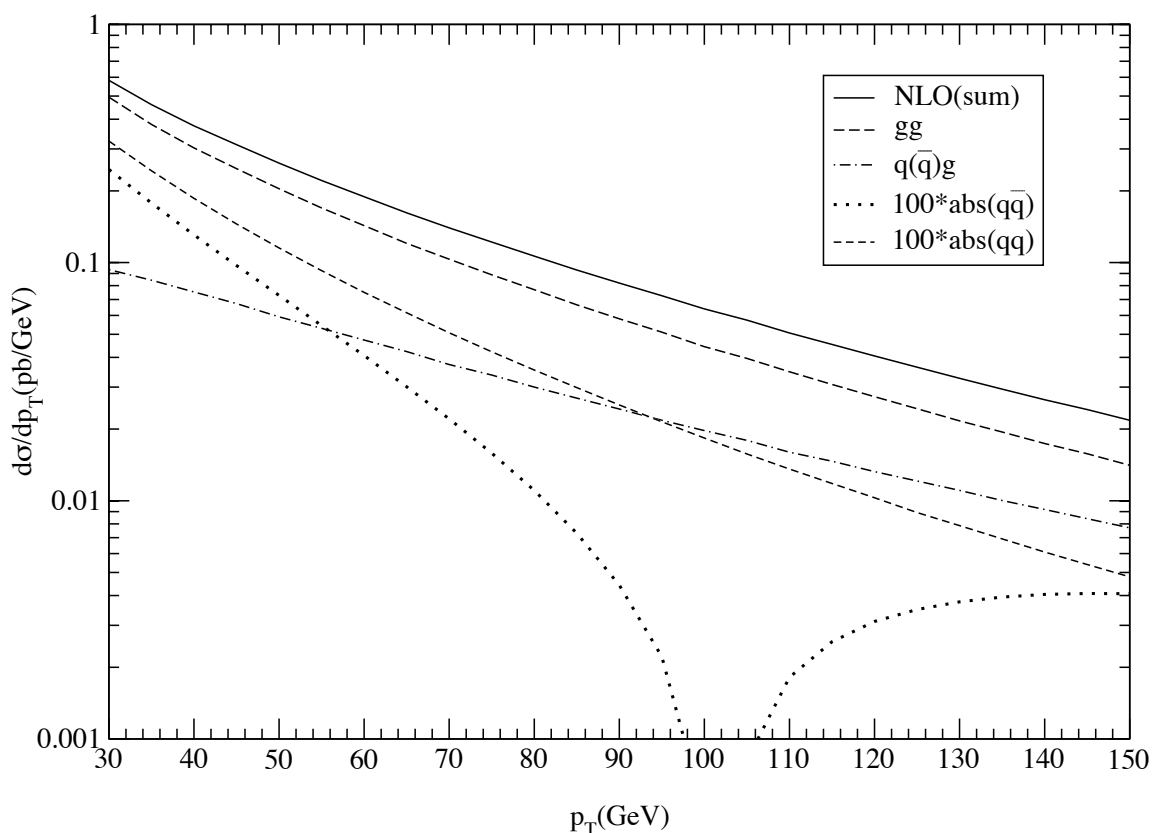
- Differential cross sections computed at NLO

deFlorian, Grazzini, Kunszt PRL 82, 5209 (1999)

Ravindran, Smith, van Neerven Nucl.Phys. B634, 247 (2002)

Glosser, Schmidt hep-ph/0209248

- gg subprocess is the largest component
- $m_h = 120 \text{ GeV}$



Ravindran, Smith, van Neerven

- The transverse momentum distribution diverges as $Q_T \rightarrow 0$ at fixed-order in perturbation theory

DIFFERENTIAL CROSS SECTION AT FIXED-ORDER IN α_s

- At fixed-order in α_s , the transverse momentum distribution behaves as

$$\frac{\alpha_s}{Q_T^2} [a + b \log(m_h^2/Q_T^2)] \rightarrow \infty \text{ as } Q_T^2 \rightarrow 0$$

- $1/Q_T^2$ divergence is related to the gluon propagator
- The logarithmic term $\log(m_h^2/Q_T^2)$ remains after the usual cancellation of infra-red divergences and the absorption of collinear divergences into the renormalized parton densities

- In addition

$$\frac{\sigma^{\text{NLO}}}{\sigma^{\text{LO}}} = \mathcal{O}(\alpha_s \log^2(m_h^2/Q_T^2)) \quad \text{is not small}$$

$$(\alpha_s(\mu)/\pi) \ln^2(m_h^2/Q_T^2) \sim 0.7$$

$$\text{if } \mu = m_h = 125 \text{ GeV and } Q_T = 14 \text{ GeV}$$

- The large logarithmic terms spoil conventional factorization in QCD perturbation theory
- The physical cross section peaks below $Q_T \sim m_h/3$. A reliable QCD calculation for small and intermediate Q_T requires that we resum the large logarithmic terms to all orders in α_s

DIFFERENTIAL CROSS SECTION AT FIXED-ORDER IN α_s

- Structure of the perturbative expansion in terms of

$\alpha_s \ln^2(Q/Q_T)$ instead of α_s

($L = \ln(Q/Q_T)$)

- $d\sigma/dQ_T^2 =$

$$Q_T^{-2} \left\{ \alpha_s ({}_1v'_1 L + {}_1v'_0) + \alpha_s^2 ({}_2v'_3 L^3 + {}_2v'_2 L^2) + \alpha_s^3 ({}_3v'_5 L^5 + {}_3v'_4 L^4) + \dots \right. \\ \left. + \alpha_s^2 ({}_2v'_1 L + {}_2v'_0 L^0) + \alpha_s^3 ({}_3v'_3 L^3 + {}_3v'_2 L^2) + \dots \right. \\ \left. + \alpha_s^3 (\dots \right.$$

- In a fixed order calculation (column by column), convergence at small Q_T is compromised by higher order uncalculated logarithmic terms
- In a resummed calculation (line by line), convergence is preserved in each “order” (each line), and higher order corrections are included systematically
- Expand the predictive power of QCD perturbation theory by (re)summing the large logarithmic contributions in an improved calculational scheme

3. ALL ORDERS SOFT GLUON RESUMMATION

- Resummation in impact parameter b -space
 - \vec{b} -space = Fourier conjugate of \vec{Q}_T -space
 - Fourier transform $\frac{d\sigma}{dydQ_T^2}$ to b -space
 - Sum multiple gluon emission to all orders in α_s
 - Transverse momentum conservation preserved
 - Fourier transform back to Q_T -space
 - Resummation produces a Q_T distribution that is finite as $Q_T \rightarrow 0$
 - Note that the perturbative region of large Q_T corresponds to small b

THE CSS b -SPACE RESUMMATION FORMALISM^a

- Resummation of logarithmic terms to all orders in b -space

$$\frac{d\sigma_{AB \rightarrow hX}}{dydQ_T^2} = \frac{d\sigma_{AB \rightarrow hX}^{(\text{resum})}}{dydQ_T^2} + \frac{d\sigma_{AB \rightarrow hX}^{(Y)}}{dydQ_T^2}$$

- $\sigma^{(\text{resum})}$: resums singular terms that diverge as $(1/Q_T^2) \ln^n(Q^2/Q_T^2)$; $n \geq 0$; $Q = m_h$
It dominates in the region of small Q_T
- $\sigma^{(Y)}$: This remainder includes all non-singular terms and may include divergences that are less singular at small Q_T . May be computed at fixed-order in α_s .
Tends to dominate at large Q_T

$$\begin{aligned} \frac{d\sigma^{(\text{resum})}}{dydQ_T^2} &= \int \frac{d^2b}{(2\pi)^2} e^{i\vec{Q}_T \cdot \vec{b}} W(b, Q) \\ &= \int \frac{db}{2\pi} J_0(Q_T b) bW(b, Q) \end{aligned}$$

- b -space distribution:

$$W(b, Q) = \sum_{ij} W_{ij}(b, Q) \sigma_{ij \rightarrow hX}^{(0)}$$

$J_0(Q_T b)$ is a Bessel function

^aJ.C. Collins, D.E. Soper, and G. Sterman, Nucl. Phys. B250, 199 (1985).

- b -space distribution for Higgs boson production

$$W(b, Q) = W_{gg}(b, Q) \sigma_{gg \rightarrow hX}^{(0)}$$

satisfies evolution equations in the region of small b :

$$\frac{\partial}{\partial \ln Q^2} W_{gg}(b, Q) = [K_g(b\mu, \alpha_s) + G_g(Q/\mu, \alpha_s)] W_{gg}(b, Q)$$

$$\frac{\partial}{\partial \ln \mu^2} K(b\mu, \alpha_s) = -\frac{1}{2} \gamma_g(\alpha_s(\mu))$$

$$\frac{\partial}{\partial \ln \mu^2} G(Q/\mu, \alpha_s) = \frac{1}{2} \gamma_g(\alpha_s(\mu))$$

- The anomalous dimension $\gamma_g(\alpha_s(\mu))$ has a perturbative expansion in powers of α_s without large logarithms
- Resummation/Solution of the homogeneous evolution equation

$$W_{gg}(b, Q) = W_{gg}(b, \frac{c}{b}) e^{-S_{gg}(b, Q)}$$

- In the perturbative region $b \ll 1/\Lambda_{\text{QCD}}$, the boundary value $W_{gg}(b, c/b)$
 - depends only on one perturbative scale $\sim 1/b$
 - contains no large logarithms
- all large logarithms are summed into $S(b, Q)$

EXPLICIT FORMULAS

$$S_g(b, Q) = \int_{c^2/b^2}^{Q^2} \frac{d\bar{\mu}^2}{\bar{\mu}^2} \left[\ln \left(\frac{Q^2}{\bar{\mu}^2} \right) A_g(\alpha_s(\bar{\mu})) + B_g(\alpha_s(\bar{\mu})) \right]$$

$$c = 2e^{-\gamma_E}$$

- A_g and B_g are free of logarithmic dependence and have well-behaved perturbative expansions:

$$A_g(\alpha_s(\bar{\mu})) = \sum_{n=1} A_g^{(n)} \left(\frac{\alpha_s(\bar{\mu})}{\pi} \right)^n$$

$$B_g(\alpha_s(\bar{\mu})) = \sum_{n=1} B_g^{(n)} \left(\frac{\alpha_s(\bar{\mu})}{\pi} \right)^n$$

$$A_g^{(1)} = C_A = N_c = 3$$

$$A_g^{(2)} = \frac{C_A}{2} \left[C_A \left(\frac{67}{18} - \frac{\pi^2}{6} \right) - \frac{5}{9} n_F \right]$$

$$B_g^{(1)} = -\frac{11C_A - 2n_F}{6}$$

$$B_g^{(2)} = C_A^2 \left(\frac{23}{24} + \frac{11}{18} \pi^2 - \frac{3}{2} \zeta(3) \right) + \frac{1}{2} C_F n_F$$

$$-C_A n_F \left(\frac{1}{12} + \frac{\pi^2}{9} \right) - \frac{11}{8} C_A C_F$$

$\zeta(3)$ is the third Riemann function; $n_F = 5$; $C_F = 4/3$

- $A_g^{(i)}$ and $B_g^{(i)}$ are larger than their fermionic counterparts; \rightarrow more soft gluon radiation in gg subprocesses

- $W_{gg}(b, c/b, x_A, x_B)$ may be written in factored form:

$$W_{gg}(b, \frac{c}{b}, x_A, x_B) = f_{g/A}(x_A, \mu, \frac{c}{b}) f_{g/B}(x_B, \mu, \frac{c}{b})$$

- $f_{g/A}$ and $f_{g/B}$ are modified gluon parton distributions:

$$f_{g/A}(x_A, \mu, \frac{c}{b}) = \sum_a \int_{x_A}^1 \frac{d\xi}{\xi} \phi_{a/A}(\xi, \mu) C_{a \rightarrow g} \left(\frac{x_A}{\xi}, \mu, \frac{c}{b} \right)$$

$\phi_{a/A}$ is a normal parton density (e.g., CTEQ, MRST)

- The short-distance coefficient functions are expanded in a perturbative series

$$C_{a \rightarrow b} \left(z, \mu, \frac{c}{b} \right) = \sum_{n=0} C_{a \rightarrow b}^{(n)}(z, \mu, b) \left(\frac{\alpha_s(\mu)}{\pi} \right)^n$$

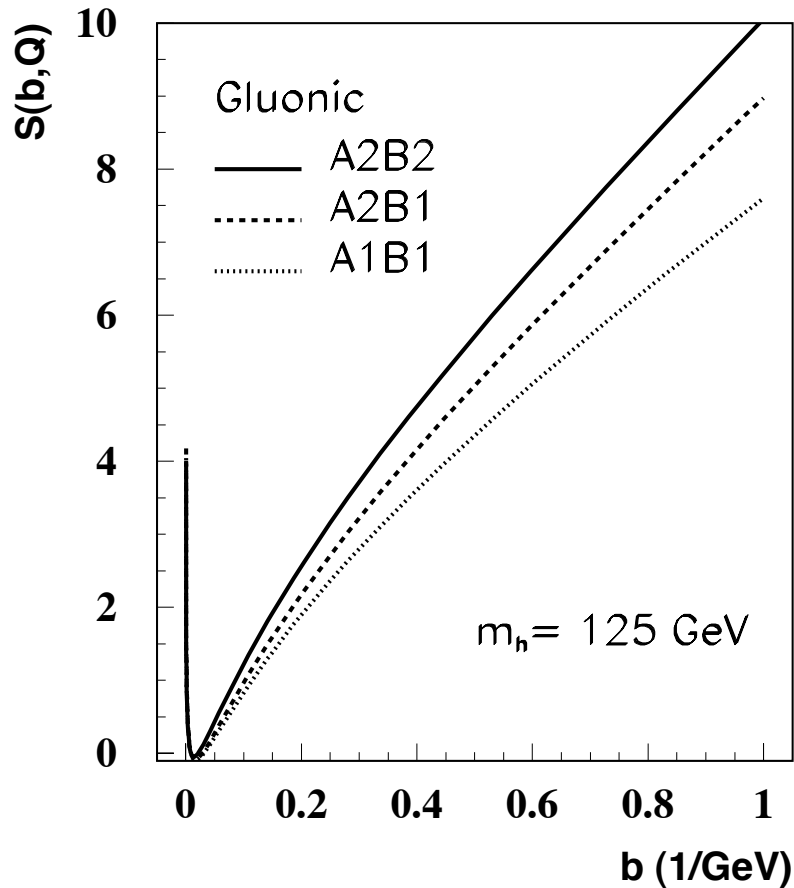
$$C_{g \rightarrow g}^{(0)}(z, \mu, \frac{c}{b}) = \delta(1 - z)$$

$$C_{i \rightarrow g}^{(0)}(z, \mu, \frac{c}{b}) = 0$$

$$C_{g \rightarrow g}^{(1)}(z, \mu, \frac{c}{b}) = \delta(1 - z) \left[C_A \left(\frac{\pi^2}{4} + \frac{5}{4} \right) - \frac{3}{4} C_F \right] - P_{g \rightarrow g}(z) \ln \left(\frac{\mu b}{c} \right)$$

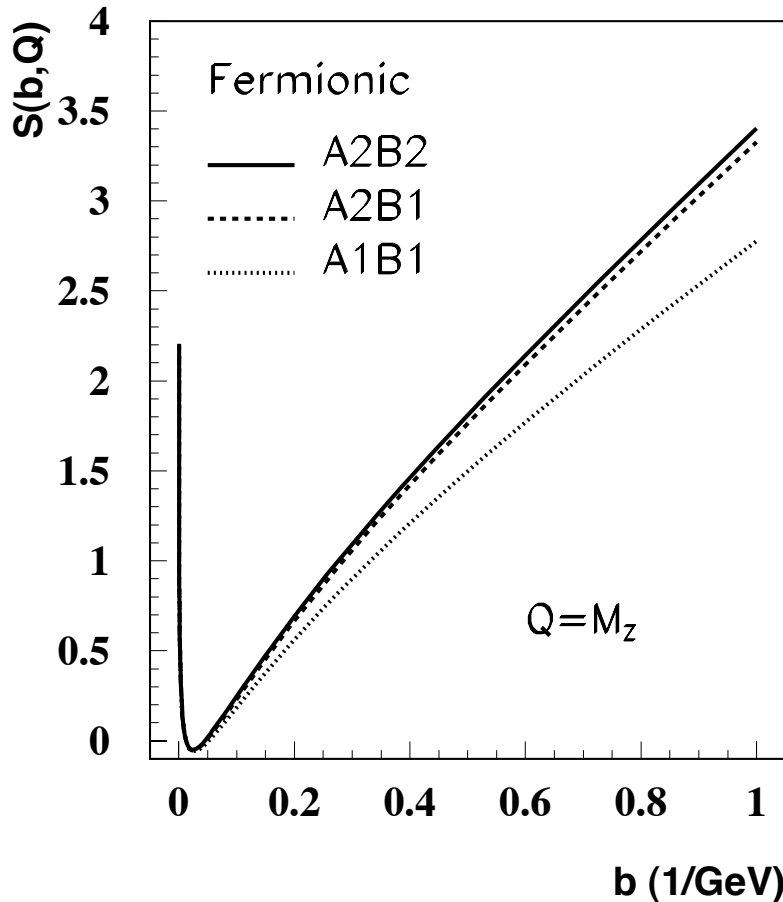
$$C_{i \rightarrow g}^{(1)}(z, \mu, c/b) = \frac{1}{2} C_F z - P_{i \rightarrow g}(z) \ln \left(\frac{\mu b}{c} \right)$$

Sudakov exponent for Higgs boson production



- The Sudakov function depends only on Q and on the perturbatively calculable functions A_g and B_g
- The function has a pronounced minimum at very small b , $b \sim 0.02 \text{ GeV}^{-1}$
- Sudakov factor strongly suppresses the regions of both large and small b
- Larger Sudakov function at large b at NLO \rightarrow the region of small Q_T is more suppressed; shift of the peak of $d\sigma/dy dQ_T$ to larger Q_T at higher orders

Sudakov exponent for Z boson production



- The Sudakov function depends only on Q and on the perturbatively calculable fermionic functions A_q and B_q
- The second-order $B_q^{(2)}$ plays a much less significant role in Z production than $B_g^{(2)}$ in Higgs boson production
- Sudakov factor $S_g(b)$ is larger than $S_q(b)$
- Larger Sudakov function at large b for the Higgs boson case \rightarrow the region of small Q_T is more suppressed; the peak of $d\sigma/dy dQ_T$ occurs at larger Q_T for the Higgs boson than for the Z boson

EXPRESSION FOR $bW(b, Q)$

- The expression in impact parameter space that includes resummation of the large logarithmic terms is $W(b, Q)$

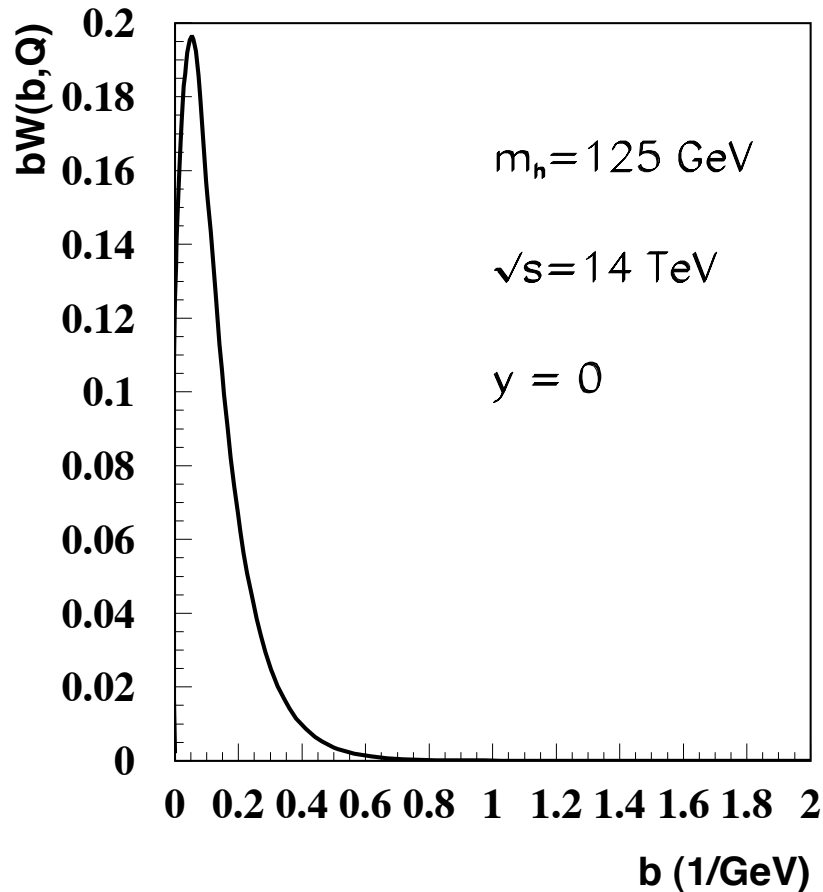
$$W(b, Q) = W(b, \frac{c}{b}) e^{-S(b, Q)}$$

- The Sudakov factor $S(b, Q)$ depends on b and Q but not on \sqrt{S}
- $W(b, c/b, x_A, x_B)$ may be written in factored form:

$$W(b, \frac{c}{b}, x_A, x_B) = f_{g/A}(x_A, \mu, \frac{c}{b}) f_{g/B}(x_B, \mu, \frac{c}{b})$$

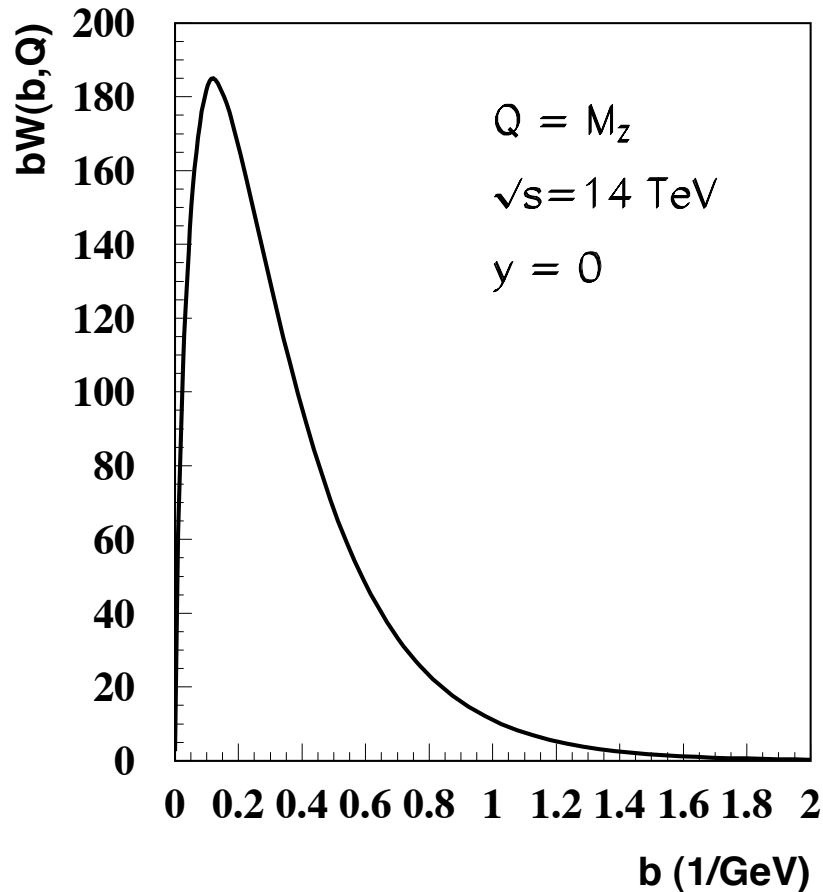
- $f_{g/A}$ and $f_{g/B}$ are modified parton distributions
- \sqrt{S} dependence enters through the parton densities

$bW(b,Q)$ for Higgs boson production



- The function is peaked sharply near $b \sim 0.05 \text{ GeV}^{-1}$ (*c.f.*, $Q_T \sim 20 \text{ GeV}$) well within the region of applicability of perturbative QCD
- The function has essentially no support for $b > 0.5 \text{ GeV}^{-1}$
- Expect, therefore, that the non-perturbative input at large b will play a negligible role in Higgs boson production at LHC energies

bW(b,Q) for Z boson production



- The function is peaked sharply near $b \sim 0.12 \text{ GeV}^{-1}$, at about twice the value for Higgs boson production (*c.f.*, $Q_T \sim 8 \text{ GeV}$) but still within the region of applicability of perturbative QCD
- The function spreads into the region $b > 1.0 \text{ GeV}^{-1}$ where non-perturbative physics may become relevant
- Expect that predictions for the Q_T distribution for the Higgs boson will be less sensitive to non-perturbative physics than those for the Z at LHC energies

RESUMMATION SCHEME

- In the CSS formalism, Sudakov exponent $S(b, Q)$ and coefficient functions $C_{i \rightarrow j}$ are process dependent
- Possible to reorganize the procedure such that these functions are universal

Catani, deFlorian, Grazzini, NP B596, 299 (2001)

- Introduce an all-orders process-dependent hard part

$H_{gg}(\alpha_s(Q))$ such that

$$W_H^{\text{pert}}(b, Q, x_A, x_B) \rightarrow \sigma_{gg \rightarrow hX}^{(0)} H_{gg}(\alpha_s(Q)) \times \sum_{a,b} [\phi_{a/A} \otimes C_{a \rightarrow g}] \otimes [\phi_{b/B} \otimes C_{b \rightarrow g}] \times e^{-S(b,Q)}$$

with

$$H_{gg}(\alpha_s(Q)) = \sum_n H_{gg}^{(n)}(\alpha_s/\pi)^n$$

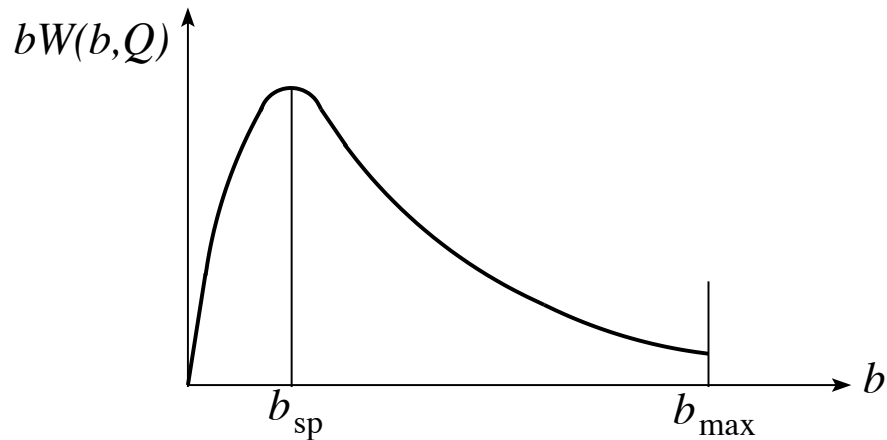
and $H_{gg}^{(0)} = 1$

- Universal $S(b, Q)$ and $C_{i \rightarrow j}$ can be defined by selecting a “resummation scheme”
- Reorganization affects only the perturbative part of $W(b, Q)$. Our approach for extrapolating into the non-perturbative region of large b could also be used in this modified approach

4. NON-PERTURBATIVE REGION OF LARGE IMPACT

PARAMETER b

- Typical form for the function $bW(b, Q)$



- Fourier transform

$$\frac{d\sigma^{(\text{resum})}}{dydQ_T^2} = \int \frac{db}{2\pi} J_0(Q_T b) bW(b, Q)$$

- $W^{\text{pert}}(b, Q)$ is valid for $b < 1/\mu_0 \sim 1 \text{ GeV}^{-1}$
- An expression is required for $bW(b, Q)$ valid for all b in order to perform the integral. Need non-perturbative input at large b

PREDICTIVE POWER OF THE RESUMMATION FORMALISM^a

- b -space distribution:

$$\int_0^\infty db J_0(Q_T b) bW(b, Q)$$

- pQCD dominates if $\int_0^{b_{max}} db(\dots) \gg \int_{b_{max}}^\infty db(\dots)$

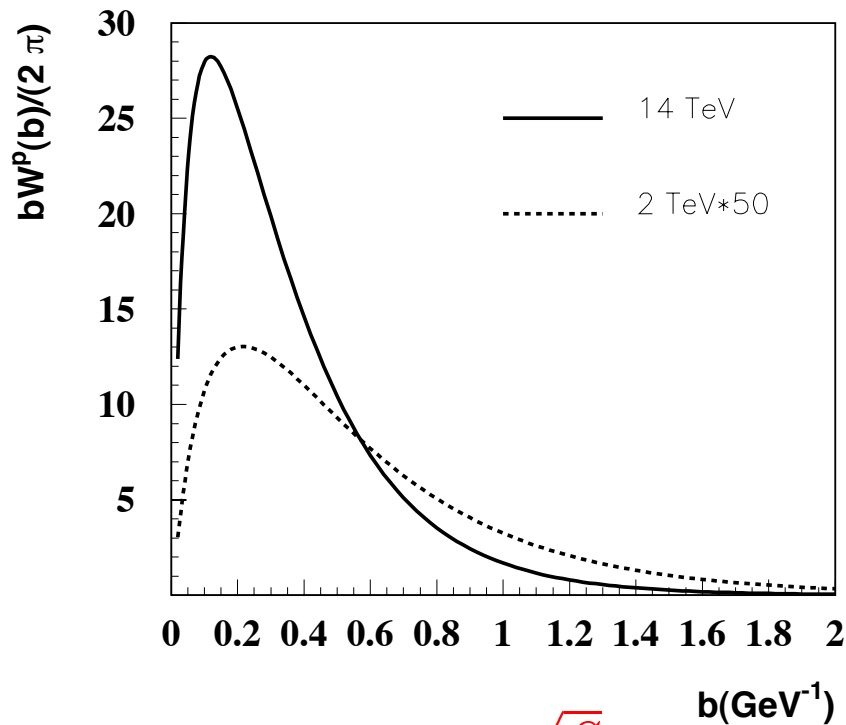
- or if the saddle point $b_{sp} \ll b_{max}$:

- b -dep of $b e^{-S(b, Q)} \rightarrow b_{sp} \propto \left(\frac{\Lambda_{\text{QCD}}}{Q}\right)^\lambda, \lambda \sim 0.6$

- b -dep of the parton densities $\phi(x, \frac{1}{b})$ from DGLAP evolution

$$\frac{d}{db} \phi(x, \frac{1}{b}) = -\frac{1}{b} \frac{d}{d \ln \frac{1}{b}} \phi(x, \frac{1}{b}) < 0 \quad \text{for } x < x_c \sim 0.1$$

Increase of $\sqrt{S} \Rightarrow$ smaller b_{sp} and narrower $bW(b, Q)$



Predictive power improves with \sqrt{S}

^a Qiu and Zhang, Phys. Rev. D63, 114011 (2001)

EXTRAPOLATION INTO THE REGION OF LARGE b

- To perform the Fourier transform

$$\frac{d\sigma^{(\text{resum})}}{dydQ_T^2} = \int \frac{db}{2\pi} J_0(Q_T b) bW(b, Q)$$

an expression is required for $bW(b, Q)$ valid for all b

- In the CSS approach a parameter b_* is introduced

$$W_{\text{CSS}}(b, Q) \equiv W^{\text{pert}}(b_*, Q) F^{NP}(b, Q)$$

- $b_* \equiv b / \sqrt{1 + (b/b_{max})^2} < b_{max} = 0.5 \text{ GeV}^{-1}$
- $F^{NP} \sim e^{-\kappa(Q, g_1, g_2, \dots)} b^2$ a Gaussian with predicted Q -dependence; fit parameters, g_1, g_2, \dots
- $F^{NP} < 1$ for all b

- The use of b_* modifies $bW(b, Q)$ even in the perturbative region

- Important effect on \sqrt{S} dependence

- $b_* < b$ for all $b \neq 0 \rightarrow$
 $W^{\text{pert}}(b_*, Q) < W^{\text{pert}}(b, Q)$ for $b < b_{\text{sp}}$ and
 $W^{\text{pert}}(b_*, Q) > W^{\text{pert}}(b, Q)$ for $b > b_{\text{sp}}$
- As \sqrt{S} increases, b_{sp} shifts down, $W^{\text{pert}}(b, Q)$ becomes narrower and steeper \rightarrow larger deviation of $W^{\text{pert}}(b_*, Q)$ from $W^{\text{pert}}(b, Q)$

QIU-ZHANG EXTRAPOLATION TO THE LARGE b REGION^a

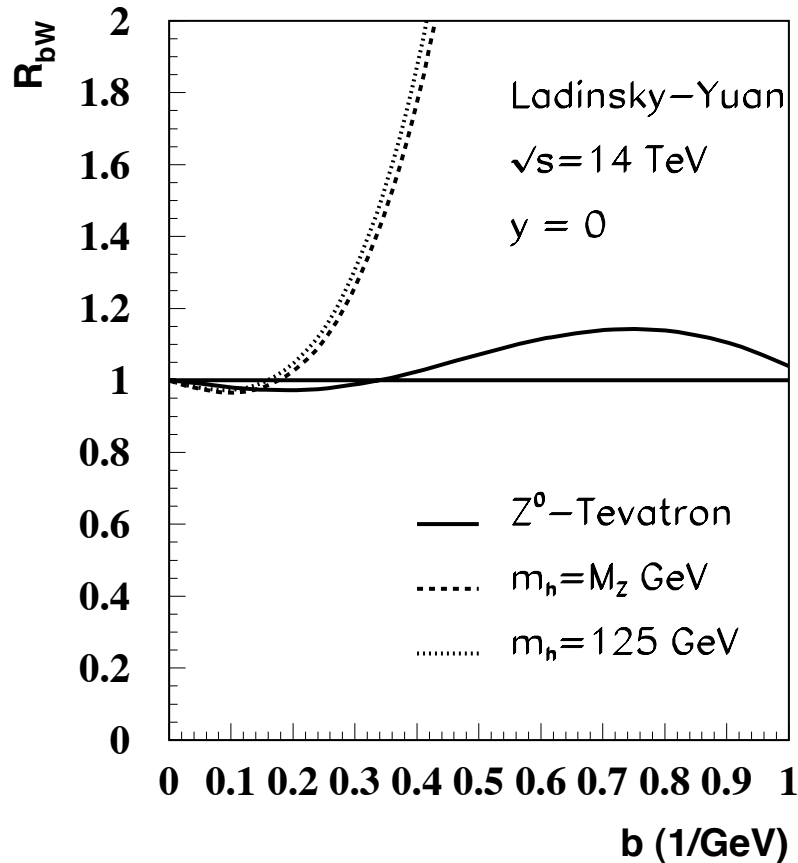
$$W(b, Q) = \begin{cases} W^{\text{pert}}(b, Q) & b \leq b_{max} \\ W^{\text{pert}}(b_{max}, Q) F^{NP}(b, Q; b_{max}) & b > b_{max} \end{cases}$$

- **Virtue:** Preserves perturbative answer for small b
- Functional form of $F^{NP}(b, Q, b_{max})$?
 - By extrapolating the resummation/evolution equations to large b , Qiu and Zhang motivate a term in $F^{NP}(b, Q; b_{max}) \propto e^{-g(b^2)^{\tilde{\alpha}}}$, with $\tilde{\alpha} < \frac{1}{2}$
 - parameters g and $\tilde{\alpha}$ are fixed by matching the b -dependence of $W(b, Q)$ at $b = b_{max}$ (1st and 2nd derivatives)
 - add $\frac{g'}{\mu^2}$ power corrections to evolution equations $\rightarrow e^{-g'(b^2)}$ Gaussian behavior for F^{NP}
 - parameter g' fixed by fitting Drell-Yan, W , Z data

$$F^{NP}(b, Q; b_{max}) = \exp \left\{ - \ln \left(\frac{Q^2 b_{max}^2}{c^2} \right) \left[g_1 \left((b^2)^{\tilde{\alpha}} - (b_{max}^2)^{\tilde{\alpha}} \right) \right. \right. \\ \left. \left. \begin{aligned} & \text{(power correction)} + g_2 \left(b^2 - b_{max}^2 \right) \\ & \text{(intrinsic p}_T\text{)} - \bar{g}_2 \left(b^2 - b_{max}^2 \right) \end{aligned} \right] \right\}$$

^a Qiu and Zhang, PRL 86, 2724(2001), PRD63, 114011(2001).

Comparison of Different Non-perturbative Forms



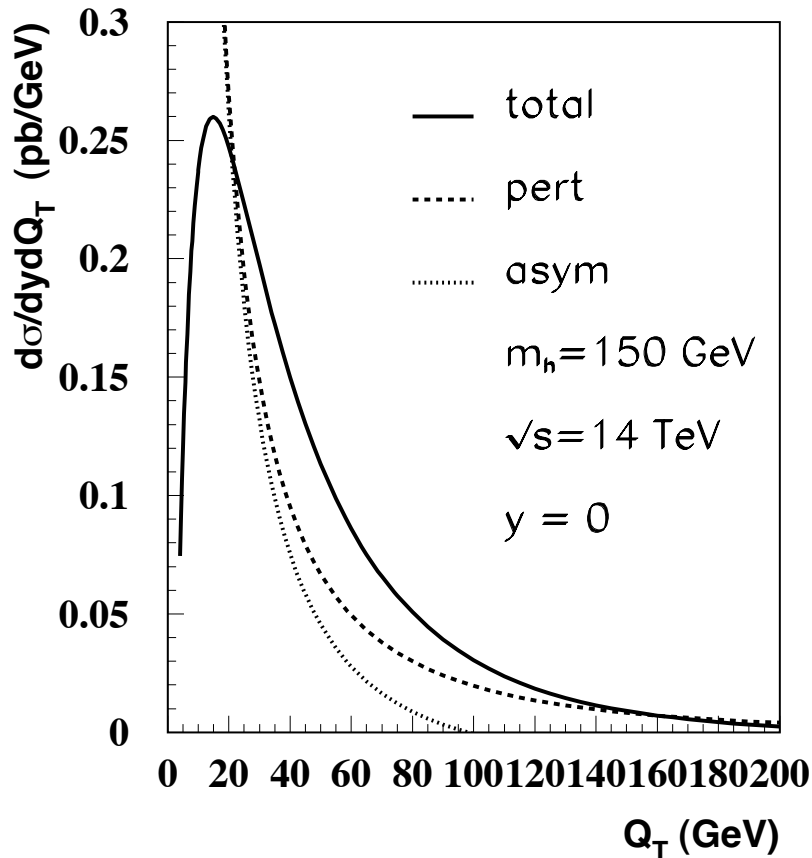
- Numerator of the ratio is the form used by Ladinsky and Yuan with the updated parameters of Landry *et al*
- Denominator is the form used by Qiu and Zhang, with $g_2 = \bar{g}_2 = 0$
- Even in the small b perturbative region, the CSS/LY form reduces the ratio for $b < 0.2$ and enhances it for $b > 0.2$
 → shift to smaller Q_T in the location of the maximum of $d\sigma/dy dQ_T$ and narrowing of the predicted peak
- Note the strong dependence on \sqrt{S}

5. PREDICTIONS

- For A_g and B_g in the Sudakov factor, use the expansion valid through second order ($n = 2$)
- For C functions, use the expansion through $n = 1$ (Results are therefore consistently at NLL accuracy).
- CTEQ5M parton densities and NLO $\alpha_s(\mu)$
- Parton-level hard-scattering functions valid through first-order in α_s
- Central value $\mu = c/b$ in the resummed term, with $c = 2e^{-\gamma_E}$; in the Y function, select a fixed scale $\mu = \kappa\sqrt{m_h^2 + Q_T^2}$, with $\kappa = 0.5$
- Extrapolation into the non-perturbative region of large b with the Qiu-Zhang form (begin with $g_2 = 0$ and $\bar{g}_2 = 0$ in F^{NP} as default choices, and then vary these)
- Integral form for the Bessel function for numerical accuracy $J_0(z) = \frac{1}{\pi} \int_0^\pi \cos(z \sin(\theta)) d\theta$
- Recall

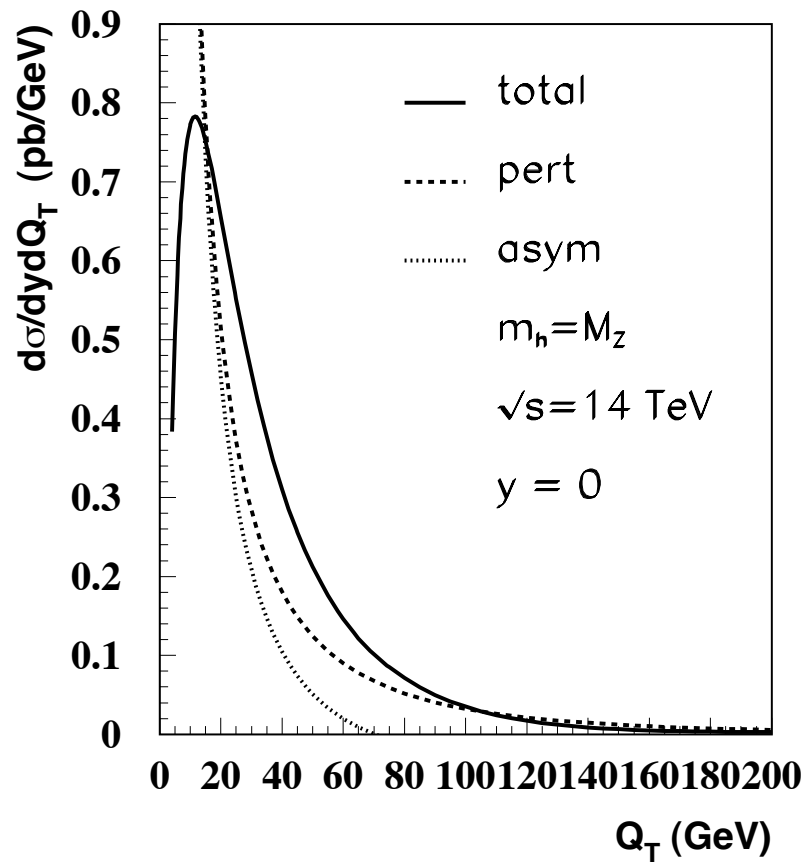
$$\frac{d\sigma_{AB \rightarrow hX}^{\text{total}}}{dydQ_T^2} = \frac{d\sigma_{AB \rightarrow hX}^{(\text{resum})}}{dydQ_T^2} + \frac{d\sigma_{AB \rightarrow hX}^{(Y)}}{dydQ_T^2}$$

Higgs boson differential cross section at LHC



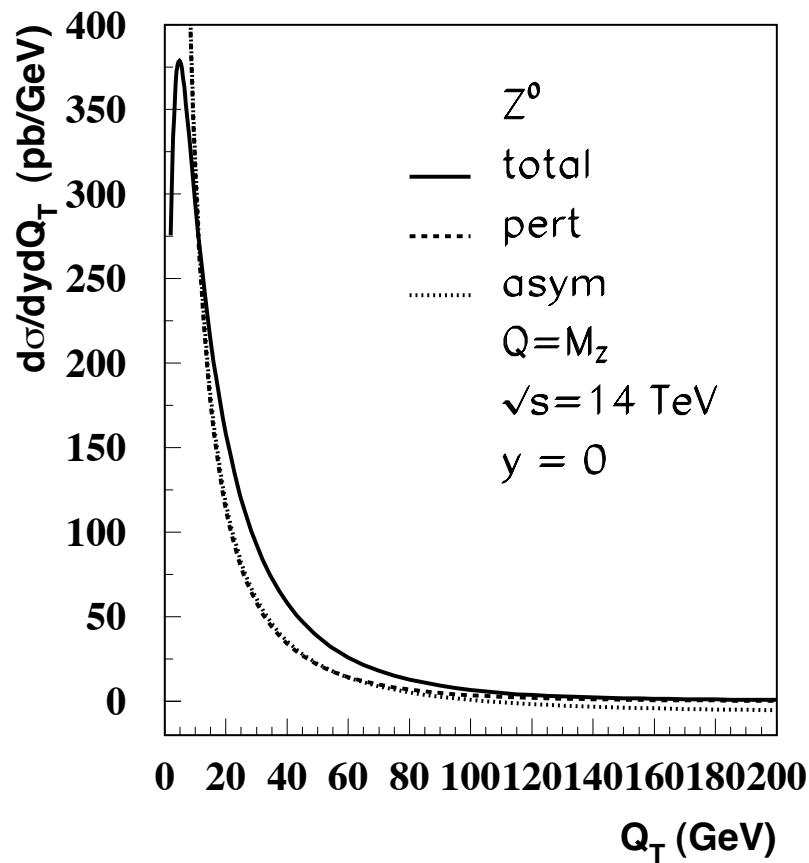
- Observe the divergence as $Q_T \rightarrow 0$ of the fixed-order perturbative result and the numerical near equality of the perturbative result and its $Q_T \rightarrow 0$ asymptotic form at small Q_T
- The total prediction is dominated by the all-orders resummed term for $Q_T \leq Q$
- The resummed result makes a smooth transition to the fixed-order perturbative result near or just above $Q_T = Q$, without need of a supplementary matching procedure, even for $d\sigma/dy dQ_T$

Higgs boson differential cross section at LHC



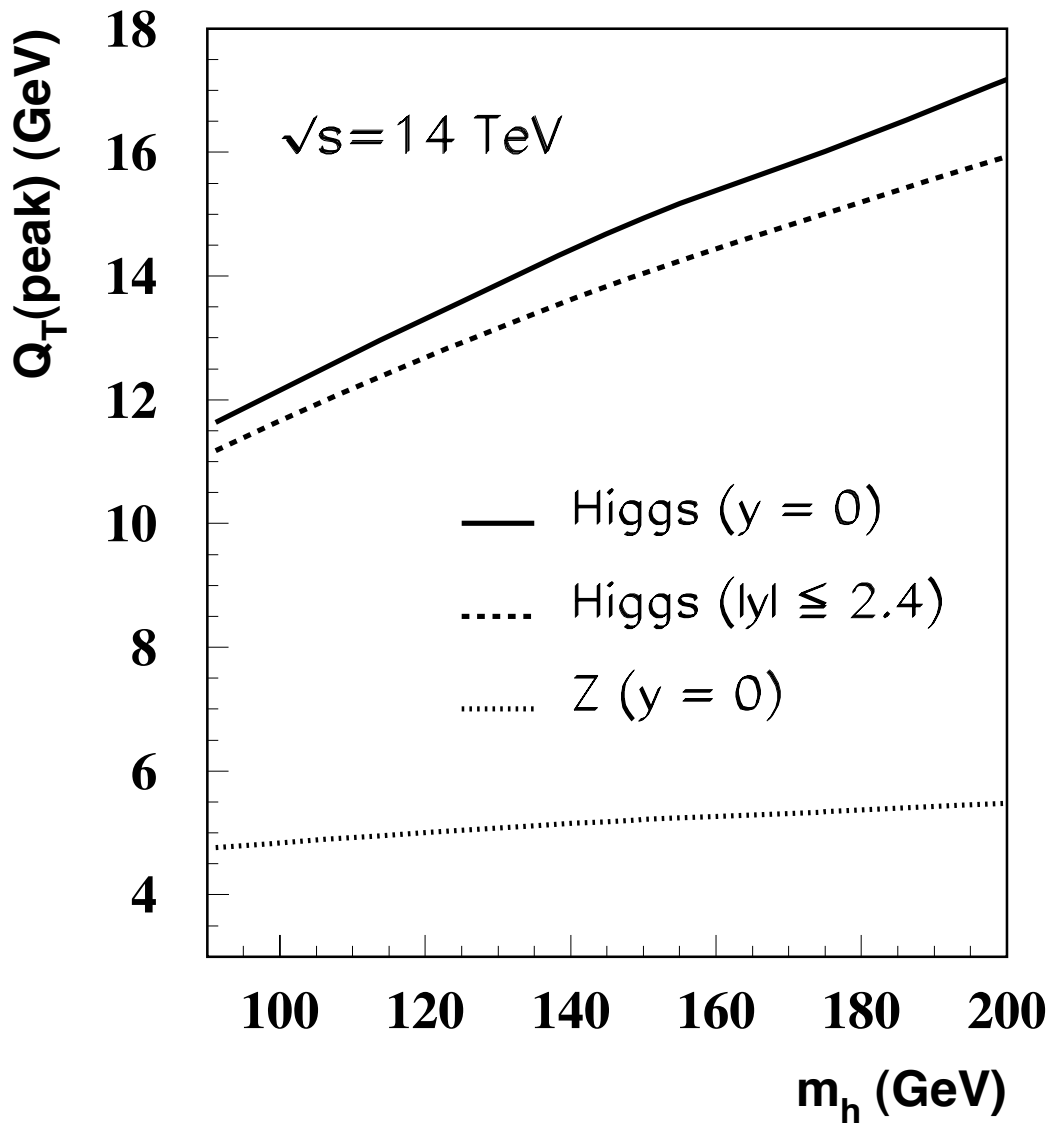
- Prediction for $m_h = M_Z$

Z boson differential cross section at LHC



- The peak occurs at a smaller value of Q_T for Z production. At $y = 0$, the peak is at $Q_T \sim 4.8$ GeV for the Z , and at $Q_T \sim 11.6$ GeV for the Higgs boson at $m_h = m_Z$
- Narrower distribution for Z production; half-maxima $Q_T \sim 16$ GeV (Z), and $Q_T \sim 35$ GeV (Higgs)
- The larger QCD color factors produce more gluonic showering in the gg subprocess that dominates Higgs boson production than in fermionic subprocesses relevant for Z production. After resummation, the enhanced showering suppresses the large- b (small Q_T) region more effectively for Higgs boson production

Peak locations in Q_T for Higgs and Z bosons at LHC

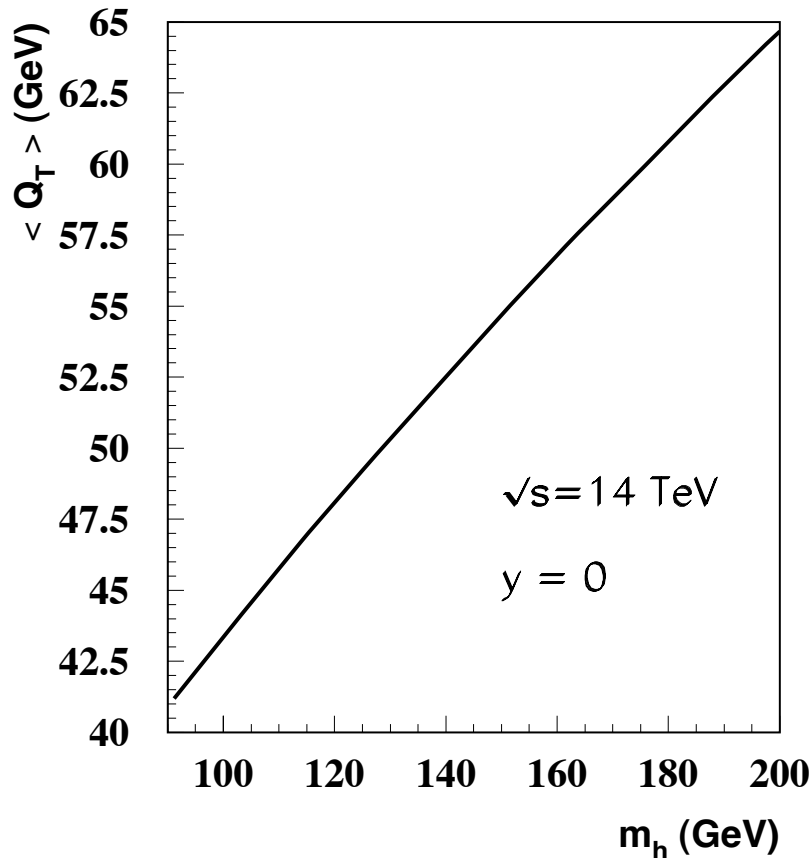


- The peak of the Q_T distribution shifts to greater Q_T as m_h grows
- For Z^* masses above M_Z , the production model is unchanged except for the difference in mass
- At $y = 0$, predict

m_h (GeV)	M_Z	125	150	200
Q_T^{peak} (GeV)	11.6	13.6	14.9	17.2

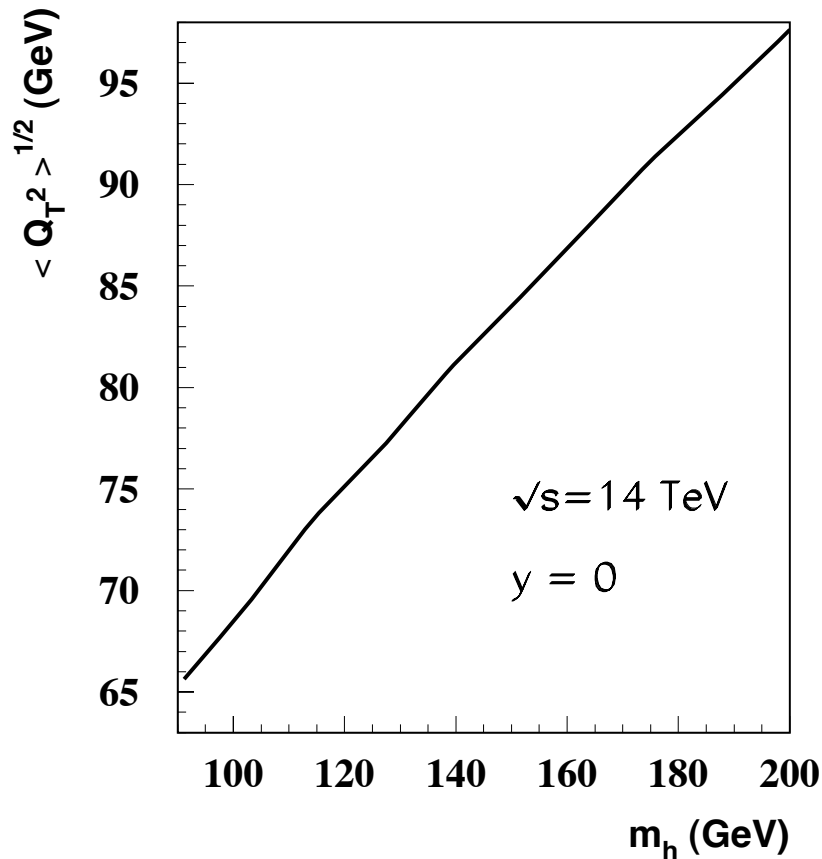
c.f. $Q_T^{\text{peak}} \simeq 11 \text{ GeV}$ at $m_h = 125 \text{ GeV}$ (Les Houches'01)

Average $\langle Q_T \rangle$ for Higgs boson production at LHC



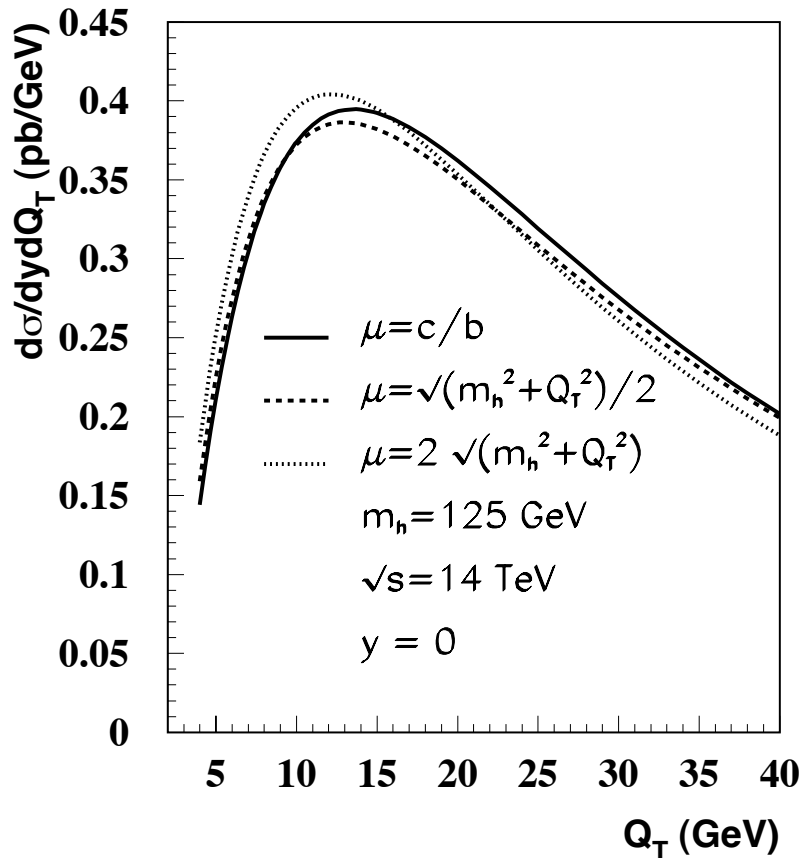
- $\langle Q_T \rangle$ grows from about 41 GeV at $m_h = M_Z$ to about 65 GeV at $m_h = 200$ GeV
- Nearly a straight line over the range shown, with $\langle Q_T \rangle \simeq 0.21m_h + 22$ GeV
- Since $Q_T \sim 1/b$, the saddle point position suggests $\langle Q_T \rangle \propto 1/b_{\text{SP}} \propto m_h^\lambda$, with fractional power λ . For large m_h , linear fit is a good approximation to fractional power dependence over a limited range in m_h .

Root-mean-square $\langle Q_T^2 \rangle^{1/2}$ for Higgs boson production



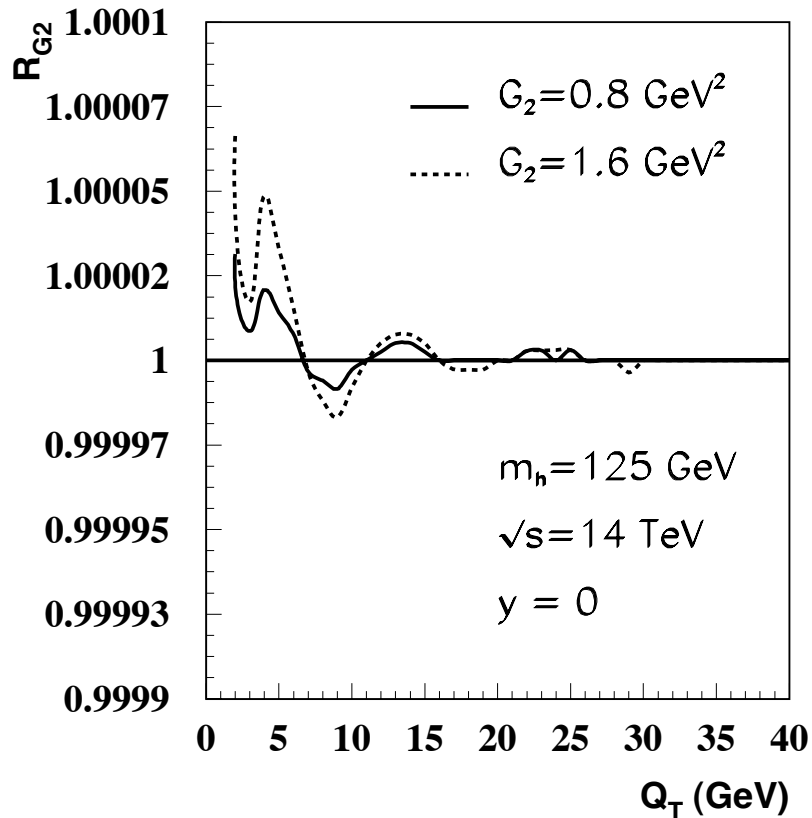
- $\langle Q_T^2 \rangle^{1/2}$ grows from about 65 GeV at $m_h = M_Z$ to about 98 GeV at $m_h = 200$ GeV
- Nearly a straight line over the range shown
- For Z production: $\langle Q_T \rangle = 25$ GeV and $\langle Q_T^2 \rangle^{1/2} = 38$ GeV. The difference $\langle Q_T^h \rangle - \langle Q_T^Z \rangle \simeq 16$ GeV at $m_h = M_Z$ is a manifestation of more significant gluonic radiation in Higgs boson production.

Renormalization/factorization scale dependence



- Default choice $\mu = c/b$ with $c = 2e^{-\gamma_E}$; scale varies with the integration variable b . Two other choices are independent of b but proportional to the hard-scale of the collision, $\mu = 0.5\sqrt{m_h^2 + Q_T^2}$ and $\mu = 2\sqrt{m_h^2 + Q_T^2}$
- Scale dependence can shift the position of the peak by about 1.5 GeV; corresponding changes in the normalization above and below the peak position. $d\sigma/dy dQ_T$ at the peak position is shifted by 4 to 5%
- Anticipate similar level of uncertainty associated with resummation scheme dependence

Dependence on parameters in the non-perturbative input



- In $G_2 = g_2 \ln(Q^2 b_{\text{max}}^2 / c^2) + \bar{g}_2$, the default choice is $g_2 = \bar{g}_2 = 0$ for Higgs production
- $G_2 = 0.4 \text{ GeV}^2$ was found to fit FNAL W and Z data best
- Results in the figure for $G_2 = 0.8 \text{ GeV}^2$ and $G_2 = 1.6 \text{ GeV}^2$ show negligible influence of the non-perturbative contributions for Higgs production. The variations are within numerical uncertainties

Scale dependence is the principal source of uncertainty.

Results are very stable except for $Q_T \ll Q_T^{\text{peak}}$

6. CONCLUSIONS AND DISCUSSION

- Subprocess $g + g \rightarrow hX$ dominates inclusive Higgs boson production at LHC with $m_h < 200$ GeV
- The two large scales m_h and Q_T and the fact that the fixed-order QCD contributions are singular as $Q_T \rightarrow 0$, necessitate all-orders resummation of large logarithmic contributions to obtain predictions for Q_T distributions
- At LHC energies, $x_A \sim x_B \sim m_h/\sqrt{S} \sim 0.009$ (for $m_h = 125$ GeV) are small, and the gluon distribution evolves steeply at small x . The saddle point in b of the Fourier transform from b -space to Q_T space is well into the region of perturbative validity
- Resummed Q_T distributions at LHC determined primarily by the perturbatively calculated b -space distributions at small b , as long as the assumed form for the non-perturbative input does not modify the resummed distribution in the perturbative region
- Predictions presented for Q_T distributions of Higgs boson and Z production at $\sqrt{S} = 14$ TeV for $m_h = M_Z$ to $m_h = 200$ GeV

- Irreducible backgrounds in the $h \rightarrow \gamma\gamma$ decay channel arise from fermionic subprocesses (e.g., $q\bar{q} \rightarrow \gamma\gamma X$; $qg \rightarrow \gamma\gamma X$) and gluonic subprocesses (e.g., $gg \rightarrow \gamma\gamma X$)
- For $M_{\gamma\gamma} = m_h$, the shape of the Q_T spectrum of the gg box contribution to the irreducible background will be the same after soft gluon resummation as that for the Higgs boson
- $q\bar{q} \rightarrow \gamma\gamma X$ subprocess, has the same initial state structure as Z production. The Q_T spectrum of the Z is softer than that for the Higgs boson because there is less gluon radiation in fermionic subprocesses
- **Suggestion** a selection of events with large $Q_T^{\gamma\gamma}$ could help to improve S/B